Electrochemical properties of Li ion polymer battery with gel polymer electrolyte based on polyurethane

H-S. KIM[1,*], G-Y. CHOI[1], S-I. MOON[1] and S-P. KIM[2]
[1]*Korea Electrotechnology Research Institute, Changwon 641-120, Korea*
[2]*Saehan Enertech Co., Chungju, Chungbuk 380-240, Korea*
(*author for correspondence, e-mail: hskim@keri.re.kr)

Abstract

Gel polymer electrolyte (GPE) was prepared using polyurethane acrylate as polymer host and its performance was evaluated. $LiCoO_2$/GPE/graphite cells were prepared and their electrochemical performance as a function of discharge currents and temperatures was evaluated. The precursor containing a 5 vol % curable mixture had a viscosity of 4.5 mPa s. The ionic conductivity of the GPE at 20 °C was about 4.5×10^{-3} S cm^{-1}. The GPE was stable electrochemically up to a potential of 4.8 V vs Li/Li$^+$. $LiCoO_2$/GPE/graphite cells showed a good high rate and low-temperature performance. The discharge capacity of the cell was stable with charge–discharge cycling.

1. Introduction

Lithium-ion polymer batteries with gel polymer electrolytes have been developed to fabricate batteries with a nonliquid leakage possibility. Many kinds of polymeric hosts such as polyacrylonitrile (PAN) [1–4], polyvinylidene fluoride (PVdF) [5], polyethylene oxide (PEO) [6–8], polymethylmethacrylate (PMMA) [9, 10] and poly (vinyl chloride) (PVC) [11] have been proposed as frameworks for gel polymer electrolytes. Their ionic conductivities were reported to be between 10^{-4} and 10^{-3} S cm^{-1} at room temperature. Hybrid polymer electrolytes based on P (VdF-HFP) [12, 13] copolymers exhibit high ionic conductivity and good mechanical performance.

Cross-linked polymers were found to reduce the solubility of the polymers in organic solvents and also helped to trap liquid electrolyte within the polymer matrix [14]. These polymers can be obtained from monomers having relatively low molecular weight and prepared by methods such as u.v., thermal radiation and electron beam radiation polymerization. Polyurethane acrylate (PUA) is one candidate for the polymer network, because it has certain merits such as compatibility with organic electrolyte, amorphous structure with low glass transition temperature and low interfacial resistance between the electrodes and the GPE.

In this work, PUA was synthesized from propylene oxide and ethylene oxide random copolymer and used as an oligomer for GPE. The precursor for GPE was prepared using PUA as a macromonomer, tri(ethylene glycol) dimethacrylate (TEGDMA) as a reactive modifier, benzoyl peroxide (BPO) as a thermal initiator and 1.0 M LiPF$_6$/EC-DEC (1:1 vol %) as the electrolyte. $LiCoO_2$/GPE/graphite cells were prepared and their electrochemical properties were evaluated at various current densities and temperatures.

2. Experimental details

The PUA was synthesized by an additional reaction of a polyol and a diisocyanate. A polyol ($M_w = 2000$, GP2000) was obtained from Hankook Polyol Co. and dehydrated under reduced pressure at 80 °C for 24 h before use. The polyol was a random copolymer of propylene oxide and ethylene oxide. Hydrogenized 4,4′-dicyclohexylmethane diisocyanate (HMDI) was obtained from Aldrich and used as received. The prepolymer was prepared by allowing the mixture of HMDI and the polyol to react at 60 °C for 2 h by stirring under a dried nitrogen blanket. After the prepolymer was synthesized, its contents of NCO groups were characterized with a dibutyl amine back titration method. Further, the required amount of hydroxyethyl acrylate (HEA) was slowly added to the NCO terminated prepolymer. The HEA was obtained from Aldrich and used as received. The reaction was allowed to continue for 3 h and then it was terminated by the addition of small amounts of methanol.

A precursor for a gel polymer electrolyte of a lithium ion polymer cell consisted of a liquid electrolyte, a macromonomer, a reactive modifier and an initiator. A curable mixture consisted of a macromonomer, a reactive modifier and an initiator. A battery grade solution of 1.0 M $LiPF_6$/EC-DEC (1:1 vol %) was obtained from Cheil Industries. TEGDMA was used as a reactive modifier to improve the mechanical properties of the gel polymer electrolyte. BPO ($C_{14}H_{10}O_4$, Aldrich Chemical Co.) was used as a thermal initiator. All procedures for preparing the precursor were carried out in a dry box filled with argon gas.

Lithium cobalt oxide electrodes were prepared by mixing 93 wt % $LiCoO_2$ (Umicore Co.) with a 4 wt % super P black and a 3 wt% PVdF and then coating onto aluminium foil. Graphite electrode were prepared using 95 wt % MCF (milled carbon fibre, Petoca Materials Co.) and a 5 wt % PVdF. Celgard 2500 was used as the separator. The electrodes were stacked and inserted into an aluminium-laminated film. The precursor was filled into the assembled cell in a dry box filled with argon gas and then it was vacuum-sealed. The assembled cells were polymerized at a temperature of 80 °C for 1 h in an oven.

The film for infrared analysis was prepared by casting the GPE onto the potassium, stored in an argon-filled dry box, and then transferred to the specimen holder in the spectrometer. FTIR spectra were collected using the Burker IFS 66/FRA 106 system at a resolution of 4 cm^{-1}. The viscosity of the precursor was measured by the DV-II$^+$ system (Brookfield Co.). The ionic conductivity of the GPE was measured using an a.c. impedance analyser (IM6, Zahner Elektrik) with a stainless steel blocking electrode cell. The ionic conductivity was measured for temperatures ranging from −20 °C to 60 °C. A potential difference of 5 mV was applied to the sample for frequencies ranging from 100 Hz to 2 MHz.

The electrochemical stability of the GPE was studied using a linear sweep voltammetry (LSV). LSV was carried out using a potentiostat (model 273, EG&G Co.) with a three-electrode system. Stainless steel was used for the working electrode and a lithium electrode was used as the counter and the reference electrode, respectively. A stainless steel electrode with an area of 3 cm × 5 cm was swept at a sweep rate of 5 mV s^{-1}. The electrochemical properties of the cell were evaluated using an a.c. impedance analyser and a cycler. A.c. impedance measurements were performed over a frequency range of 700 mHz to 2 MHz for an interface investigation of the cells. The charge and discharge cycling tests of the $LiCoO_2$/GPE/graphite cells were conducted galvanostatically using the Toyo battery test system (TOSCAT-3100K). The discharge curves were obtained at different current rates in order to obtain the rate capability of the cell and also at various temperatures to determine low-temperature performance.

3. Results and discussion

Figure 1 showed the typical i.r. spectrum obtained from polyurethane acrylate. There were many peaks such as the N–H stretching region at wavenumber about 3600 cm^{-1}, the aliphatic C–H stretching region at wavenumber about 3000–2900 cm^{-1}, and the carbonyl group's peak at wavenumber about 1800–1700 cm^{-1} on the spectrum.

The viscosity of the precursor is one of the important factors to consider in a gel-type lithium-ion polymer battery, because electrodes and separator have to be wetted sufficiently to show good cell performance. Figure 2 showed the relationship between the contents of the liquid electrolyte and the viscosity of the precursor. The viscosity of the precursor containing a 40 vol% monomer was about 32 mPa s and decreased with decreasing the contents of the curable mixture. The viscosity of the precursor containing a 5 vol% curable mixture was around 4.5 mPa s and it was nearly same level in the liquid electrolyte.
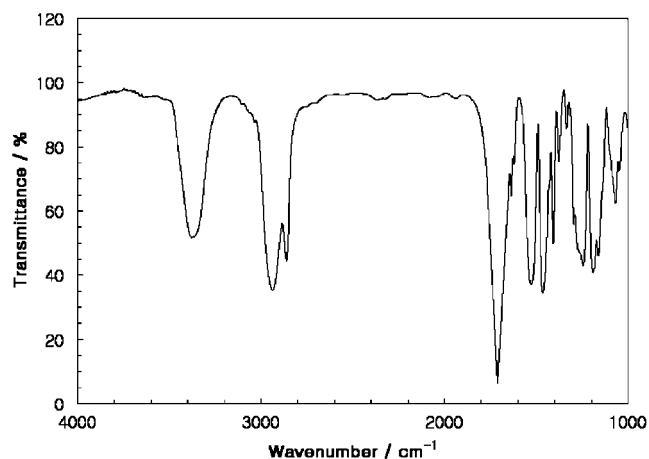

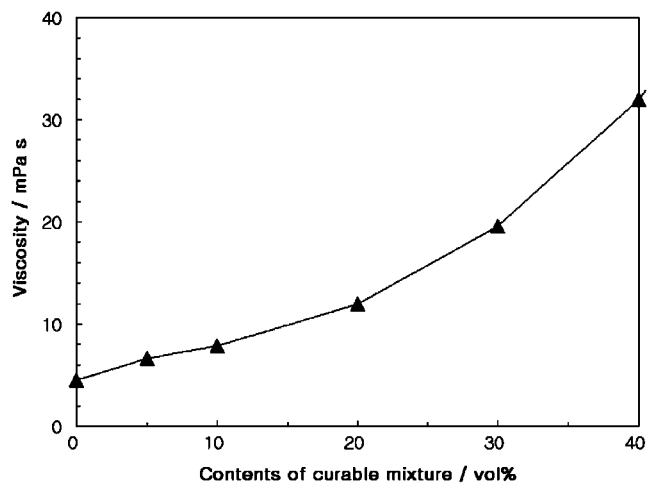Fig. 1. FTIR spectrum of polyurethane acrylate macromonomer.

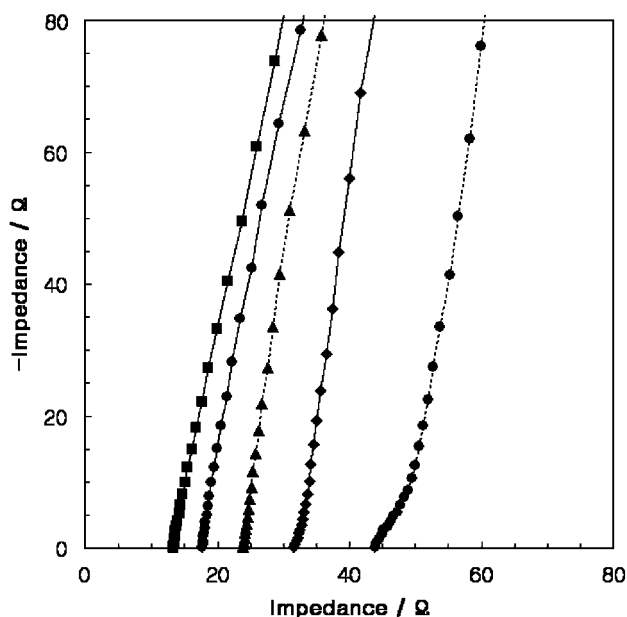Fig. 2. Relationship between the viscosity of the precursor and the contents of the curable mixture.

Fig. 3. A.c. impedance spectra of SS/GPE/SS cell with gel polymer electrolyte. Temperature: (■) 40, (●) 20, (▲) 0, (♦) −10 and (···●···) −20 °C.

Fig. 4. Ionic conductivity of gel polymer electrolyte obtained at various temperatures.

The ionic conductivity is most important factor in the gel polymer electrolyte. It has been reported that the ionic conductivity [2–4] of the membrane-type gel polymer electrolyte is about 10^{-4} S cm^{-1}. Figure 3 showed the a.c. impedance spectra of the GPEs polymerized at a temperature of 80 °C for 1 h. There was only a spike, which represents a resistor in series with a capacitor, on the plot [15]. The intercept on the real axis gives the resistance of the GPE. The ionic conductivity at 20 °C was calculated to be 5.9×10^{-3} S cm^{-1} from the electrolyte resistance with the thickness and surface area of the GPE. The full linearity in the high frequency region is convincing evidence of the integrity of the gel polymer. If phase separation and/or crystallization had been present, these would have been evidenced by the appearance of semicircles or, more generally, by deviation from linearity in the high frequency region of the impedance spectra [16]. It was, therefore, thought that crystallization in the gel polymer occurred at around −20 °C because deviation from linearity in the high frequency region was observed.

The performance of lithium-ion polymer batteries at low temperature and high current is low compared with lithium-ion batteries with liquid electrolyte. Figure 4 showed the ionic conductivity of the GPE containing a 5 vol% curable mixture obtained at various temperatures. To be compared, the ionic conductivity of the liquid electrolyte was also plotted. The ionic conductivity of GPE at 20 °C was around 4.5×10^{-3} S cm^{-1} and it was even 1.1×10^{-3} S cm^{-1} at a temperature of −20 °C. Further, it increased with increase in temperature. This behavior can be rationalized by recognizing the free-volume model [17]. As the temperature increases, the polymer can expand easily and produce free volume. Thus, ions, solvated molecules, or polymer
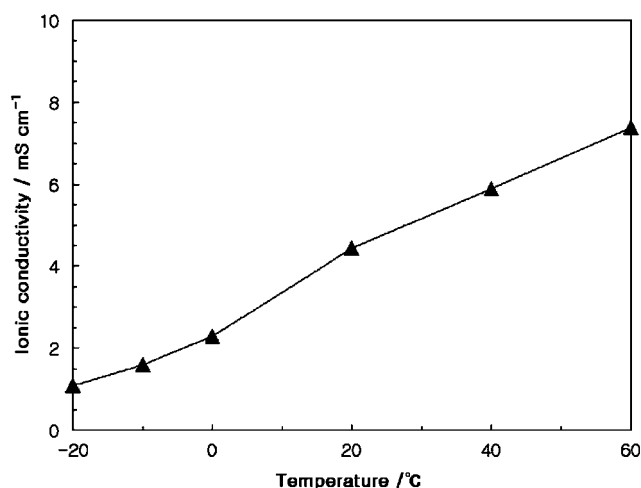
segments can move into the free volume. The resulting conductivity, represented by the overall mobility of ion and polymer, was determined by the free volume around the polymer chains. Therefore, as temperature increases, the free volume increases. This leads to an increase in ion mobility and segmental mobility that will assist the ion transport and virtually compensate for the retarding effect of the ion clouds.

In a lithium ion polymer battery using the GPE, it is required that the mechanical property is considered as well as the mobility of the lithium ion. The TEGDMA was used to obtain a dense network structure and to decrease the viscosity of the polyurethane acrylate. Figure 5 showed the relationship between the ionic conductivity of lithium ions and the contents of the TEGDMA. The ionic conductivity decreased with increasing TEGDMA contents. Gelation time decreased and the whitening phenomena were observed in the gelation test when the contents of the TEGDMA were increased. Mechanical stability might be enhanced by adding the reactive modifier because the ionic conductivity
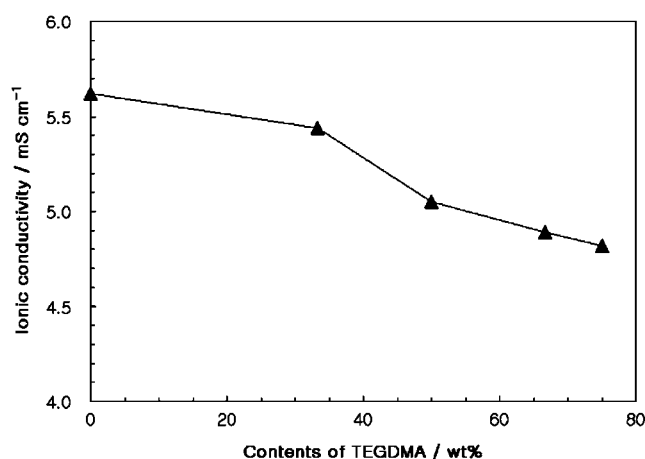

Fig. 5. Relationship between the ionic conductivity of GPE and the contents of TEGDMA.

and the mechanical stability were in a trade-off relationship; however, mechanical strength tests were not performed in this study.

The electrochemical stability of the GPE was studied using linear sweep voltammetry. Figure 6 showed the voltammograms of the GPE on the stainless steel electrodes. The decomposition voltage was observed at around 4.8 V vs Li/Li^+. There is no problem in the electrochemical stability of the GPE, because the charging voltage for a lithium ion battery using lithium cobalt oxide is about 4.2 V.

Figure 7 shows the a.c. impedance spectra of the $LiCoO_2$/GPE/graphite cell. The impedance spectrum of the cell was obtained after filling of the precursor and the 1st cycling. Only one semicircle was observed at a higher frequency in a cell that was not cycled, which is related to the bulk resistance (R_b) of the GPE. After the 1st cycling, the impedance spectroscopy of the cell

exhibited two depressed semicircles. The Z' intercept of the semicircle on the real axis at higher frequency is related to the bulk resistance of the GPE. The semicircle was assumed to be associated with a parallel combination of interfacial resistance (R_{int}) and the capacitance of the passivation film on both electrode surfaces [18]. The diameter of the semicircle is related to the interfacial resistance between the electrode and the GPE [19]. The semicircle at medium frequency is assigned to the parallel combination of the charge transfer resistance (R_{ct}) in the electrodes and the double-layer capacitance (C_{dl}) contributed by both the cathode and the anode. At a lower frequency there is a slanted line due to the solid-state diffusion of lithium ions within the bulk cathode/anode materials.

To evaluate electrochemical performance of a lithium-ion polymer battery, $LiCoO_2$/GPE/graphite cells were fabricated. The GPE consisted of a 5 vol% curable mixture and a 95 vol% 1.0 M $LiPF_6$/EC-DEC. The cell was preconditioned with a cut-off voltage of 4.2 V for the upper limit and 3.0 V for the lower limit at the 0.2C rate (0.5 mA cm^{-2}). An irreversible capacity was observed in the 1st cycle, caused by the formation of a passive film on the surface of the graphite electrode due to electrolyte decomposition, as reported previously [20, 21]. The surface passivation during the initial cycling is referred to as the formation period. This film is a lithium ion conductor and an electronic insulator with characteristics preventing further reduction and thus limits the electrolyte degradation.

After the preconditioning cycle, the cell was charged and discharged at various current densities and temperatures. The charge and discharge curves of the cell showed a well-defined charge–discharge voltage profile, which indicates reversible cycling. The small voltage drop in the cycle test confirms the low internal resistance of the lithium-ion polymer cell. The coulombic efficiency in the cycle test was about 100%. The discharge curves obtained at different current rates are given in Figure 8. The cell delivered a specific discharge capacity of about
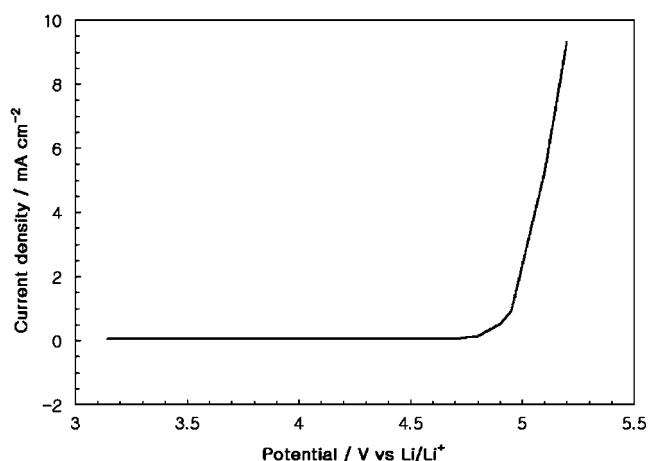

Fig. 6. Linear sweep of stainless steel/GPE/Li cell at 20 °C. Counter electrode: Li metal foil; working electrode: stainless steel; reference electrode: Li method foil. Sweep rate 5 mV s^{-1}.
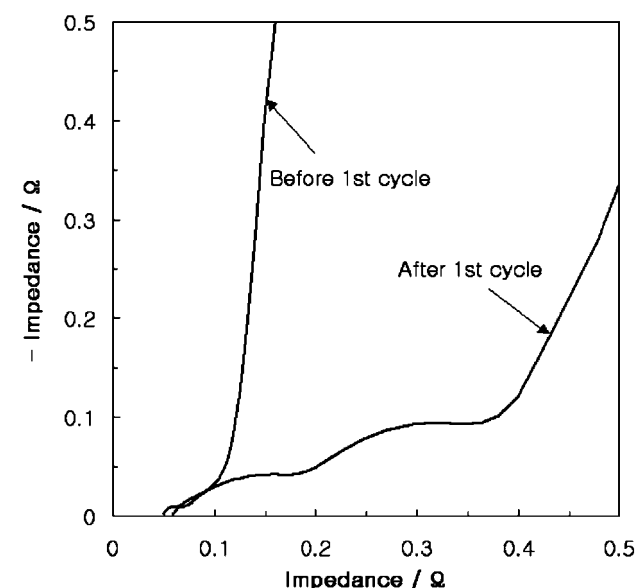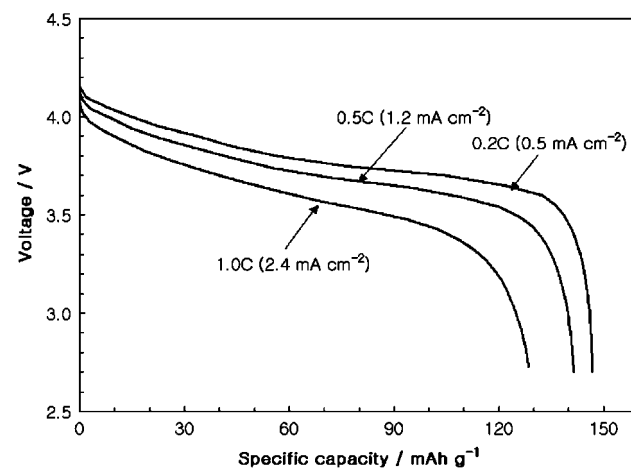

Fig. 7. A.c. impedance spectra of $LiCoO_2$/GPE/graphite cell at 20 °C.

Fig. 8. Typical discharge curves for $LiCoO_2$/GPE/MCF cell at various current densities at 20 °C.

147 mAh g^{-1} at a current density of 0.5 mA cm^{-2} (0.2C rate). The specific capacity was calculated from the weight of the cathode material. The specific capacity slowly decreased with the discharge rate, due to polarization. A useful capacity of about 141 mAh g^{-1} was obtained at a 0.5C rate, which was 96% of the discharge capacity at the 0.2C rate. The capacity of about 129 mAh g^{-1} was available even at the 1.0C rate, which was 88% of the discharge capacity at the 0.2C rate. The reduced capacity in the cell at high rate may be primarily related to the lower diffusion rate of lithium ions in the gel polymer electrolyte [22].

The performances of the LiCoO$_2$/GPE/graphite cell at various temperatures were also evaluated. The discharge curves obtained at the current density of 1.2 mA cm^{-2} (0.5C rate) at various temperatures are given in Figure 9. The specific discharge capacity slowly decreased with decreasing temperature. A useful capacity of about 415 mAh was obtained at −10 °C, which was 85% of the discharge capacity at 20 °C. Recently, ethyl methyl carbonate was found to be a useful cosolvent in binary solutions with propylene carbonate and ethylene carbonate, because of its low freezing point. Propylene carbonate is also one of the solvents that shows good low-temperature performance. Therefore, performances of the lithium-ion cells at low temperature can be improved using such solvents having a low freezing point.

Figure 10 shows the discharge capacity of the cycling of the LiCoO$_2$/GPE/graphite cell at a current density of 1.2 mA cm^{-2} (0.5C rate). The discharge capacity of the cell was stable and decreased slightly with charge-discharge cycling. This decline in capacity was primarily due to loss of interfacial contact between the electrodes and the GPE upon cycling, which gradually increases the internal resistance of the cell [23]. Furthermore, it is also reported that cross-linking polymers after curing decrease the interface resistance between the electrodes and gel polymer electrolytes [14].
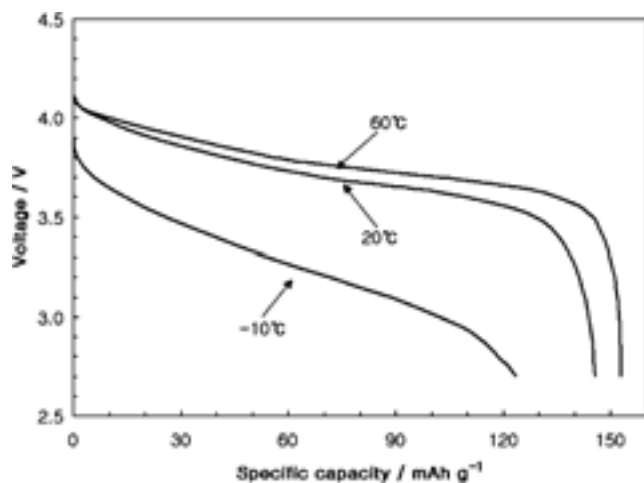

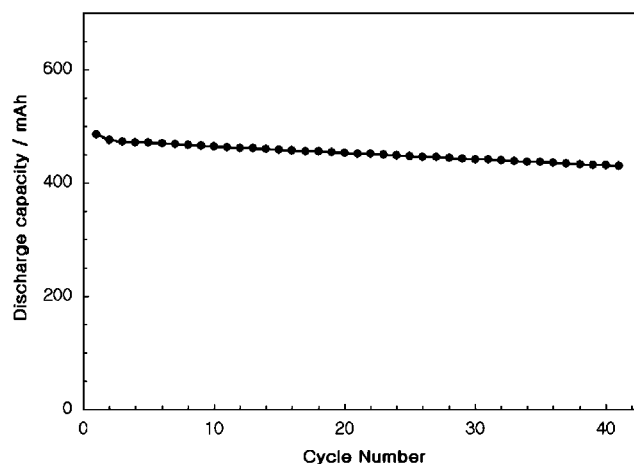*Fig. 9.* Typical discharge curves for LiCoO$_2$/GPE/MCF cell at various temperatures.

Fig. 10. Discharge capacity upon cycling at current density of 1.2 mA cm^{-2} for LiCoO$_2$/GPE/graphite cell at 20 °C.

4. Conclusions

The GPE was prepared using PUA, TEGDMA and a liquid electrolyte. The viscosity of the precursor containing the 5 vol % curable mixture was around 4.5 mPa s. The ionic conductivity of the GPE at 20 °C was around 4.5 × 10^{-3} S cm^{-1}. The GPE had good electrochemical stability up to 4.8 V vs Li/Li$^+$. The capacity of the LiCoO$_2$/GPE/graphite cell at the 1.0C rate was 88% of the discharge capacity at the 0.2C rate. The discharge capacity slowly decreased with decreasing temperature. The capacity of the cell at a temperature of −10 °C was 85% of the discharge capacity at a temperature of 20 °C. The discharge capacity of the cell with the GPE was stable with charge-discharge cycling.

References

1. K.M. Abraham and M. Alamgir, *J. Electrochem. Soc.* **136** (1990) 1657.
2. D. Kim, K. Noh, H. Min, D. Kang and Y. Sun, *Electrochem. & Solid-State Lett.* **5** (2002) A63.
3. H. Akashi, K. Tanaka and K. Sekai, *J. Power Sources* **104** (2002) 241.
4. S. Panero, D. Satolli, A. D'Epifano and B. Scrosati, *J. Electrochem. Soc.* **149** (2002) A414.
5. F. Boudin, X. Andrieu, C. Jehoulet and I.I. Olsen, *J. Power Sources* **81–82** (1999) 804.
6. B. Scrosati, F. Croce and L. Persi, *J. Electrochem. Soc.* **147** (2000) 1718.
7. Y. Aihara, G.B. Appetecchi and B. Scrosati, *J. Electrochem. Soc.* **149** (2002) A849.
8. M. Kono, E. Hayashi and M. Watanabe, *J. Electrochem. Soc.* **146** (1999) 1626.
9. E. Quartarone, C. Tomasi, P. Mustarelli, G.B. Appetecchi and F. Croce, *Electrochim. Acta* **43** (1998) 1435.
10. S. Kuwabata and M. Tomiyori, *J. Electrochem. Soc.* **149** (2002) A988.
11. M. Alamgir and K.M. Abraham, *J. Electrochem. Soc.* **140** (1993) L96.
12. V. Arcella, A. Sanguineti, E. Quartane and P. Mustarelli, *J. Power Sources* **81–82** (1999) 790.
13. H. Huang and S.L. Wunder, *J. Electrochem. Soc.* **148** (2001) A279.
14. H. Kim, J. Shin, C. Doh, S. Moon and S. Kim, *J. Power Sources* **112** (2002) 469.

496

15. G.G. Kumar and N. Munichandraiah, *J. Power Sources* **102** (2001) 46.
16. W.A. van Schalkwijk and B. Scrosati (Eds), 'Advances in Lithium-Ion Batteries' (Kluwer Academic/Plenum Publishers, New York, 2002).
17. S. Rajendran and T. Uma, *J. Power Sources* **88** (2000) 282.
18. M.D. Levi, G. Salitra, B. Makovsky, H.D. Abache, U. Heider and L. Heider, *J. Electrochem. Soc.* **146** (1999) 1279.
19. H. Wang, H. Huang and S.L. Wunder, *J. Electrochem. Soc.* **147** (2000) 2853.
20. R. Fong, U. von Sacken and J.R. Dahn, *J. Electrochem. Soc.* **137** (1990) 2009.
21. J.M. Tarascon and D. Guyomard, *J. Electrochem. Soc.* **138** (1991) 2864.
22. D. Kim, *J. Power Sources* **87** (2000) 78.
23. D. Kim and Y. Sun, *J. Power Sources* **102** (2001) 41.